Cardiovascular Research (2008) **80**, 20–29
doi:10.1093/cvr/cvn161

Phosphoproteome analysis of isoflurane-protected heart mitochondria: phosphorylation of adenine nucleotide translocator-1 on Tyr^{194} regulates mitochondrial function

Jianhua Feng[1], Min Zhu[1], Marcus C. Schaub[2], Peter Gehrig[3], Bernd Roschitzki[3], Eliana Lucchinetti[1†], and Michael Zaugg[1†*]

[1]*Cardiovascular Anesthesia Research Laboratory, Institute of Anesthesiology, E-HOF, University Hospital Zurich, Switzerland, and Center of Integrative Human Physiology, University of Zurich, Rämistrasse 100, CH-8091 Zurich, Switzerland;* [2]*Institute of Pharmacology and Toxicology, University of Zurich, Switzerland; and* [3]*Functional Genomics Center Zurich, Swiss Federal Institute of Technology Zurich and University of Zurich, Switzerland*

Received 2 April 2008; revised 6 June 2008; accepted 10 June 2008; online publish-ahead-of-print 16 June 2008

Time for primary review: 22 days

KEYWORDS
Preconditioning;
Ischaemia/reperfusion;
Adenine nucleotide translocator;
Protein phosphorylation

Aims Reversible phosphorylation of mitochondrial proteins is essential in the regulation of respiratory function, energy metabolism, and mitochondrion-mediated cell death. We hypothesized that mitochondrial protein phosphorylation plays a critical role in cardioprotection during pre and postconditioning, two of the most efficient anti-ischaemic therapies.

Methods and results Using phosphoproteomic approaches, we investigated the profiles of phosphorylated proteins in Wistar rat heart mitochondria protected by pharmacological pre and postconditioning elicited by isoflurane. Sixty-one spots were detected by two-dimensional blue-native gel electrophoresis-coupled Western blotting using a phospho-Ser/Thr/Tyr-specific antibody, and 45 of these spots were identified by matrix-assisted laser desorption/ionization-time of flight mass spectrometry. Eleven protein spots related to oxidative phosphorylation, energy metabolism, chaperone, and carrier functions exhibited significant changes in their phosphorylation state when protected mitochondria were compared with unprotected. Using a phosphopeptide enrichment protocol followed by liquid chromatography-MS/MS, 26 potential phosphorylation sites were identified in 19 proteins. Among these, a novel phosphorylation site was detected in adenine nucleotide translocator-1 (ANT1) at residue Tyr^{194}. Changes in ANT phosphorylation between protected and unprotected mitochondria were confirmed by immunoprecipitation. The biological significance of ANT phosphorylation at Tyr^{194} was further tested with site-directed mutagenesis in yeast. Substitution of Tyr^{194} with Phe, mimicking the non-phosphorylated state, resulted in the inhibition of yeast growth on non-fermentable carbon sources, implying a critical role of phosphorylation at this residue in regulating ANT function and cellular respiration.

Conclusions Our analysis emphasizes the regulatory functions of the phosphoproteome in heart mitochondria and reveals a novel, potential link between bioenergetics and cardioprotection.

1. Introduction

Pre and postconditioning are two of the most effective measures against myocardial infarction, reducing infarct size by up to 70%. Ischaemic preconditioning, first described in 1986,[1] is a biological process, whereby a transient stressful stimulus induces a protective state against a more prolonged, potentially lethal insult. It can be induced by brief ischaemic episodes or by pharmacological means.[2] In contrast, postconditioning, first reported in 2003,[3] is a process whereby ischaemic heart damage is markedly reduced through brief cycles of alternating ischaemia and reperfusion or administration of specific drugs right at the onset of reperfusion. Despite having location at the opposite sites of ischaemia, pre and postconditioning share numerous signalling pathways,[4] including the so-called reperfusion injury salvage kinases ('RISK'), protein kinase B/Akt and p42/44 extracellular signal-regulated kinase 1/2, which converge at the mitochondrial level preventing permeability transition through

† Both authors equally contributed to this work.
* Corresponding author. Tel: +41 44 255 46 00; fax: +41 44 255 44 09.
E-mail address: michael.zaugg@usz.ch

phosphorylation and inhibition of glycogen synthase kinase-3β,[5] by an yet unknown mechanism.

Mitochondria plays a central role in ischaemia-reperfusion damage of the heart[6–8] and hence, are promising targets for novel anti-ischaemic therapies. These complex double membrane-enclosed organelles are not only responsible for ATP production but are also involved in the regulation of cell metabolism, differentiation, Ca^{2+} homeostasis, and death signalling. To meet the dynamic cellular requirements, mitochondrial function must be tightly and rapidly regulated. An increasing body of evidence points to protein phosphorylation as the key regulatory mechanism responsible for mitochondrial regulation.[9] Indeed, various kinases, namely protein kinase A, B, C, and G, mitogen-activated protein kinases, glycogen synthase kinase-3β, hexokinase, creatine kinase 2, Src kinase family members were identified in or in close association with mitochondria.[9–13] Although recent studies shed new light on the role of phosphorylation as an important post-translational modification in respiratory chain proteins of heart mitochondria,[14–17] only a limited number of phosphoproteins have been characterized so far.

The aim of this study was to determine the phosphoprotein profiles of pre and postconditioned, i.e. protected heart mitochondria using proteomics analysis and to compare these with the profile of unprotected mitochondria exposed to ischaemia-reperfusion alone. This could ultimately unravel novel phosphorylation sites potentially involved in cardioprotection. Using site-directed mutagenesis in the yeast, an established model of mitochondrial function, the biological significance of one of the newly detected phosphorylation sites, namely Tyr^{194} of the adenine nucleotide translocator-1 (ANT1), could be confirmed. Our study adds a new aspect to the mechanisms underlying cardioprotection and points to the importance of mitochondria in this context.

2. Methods

An expanded Methods section is available in the online data supplement.

2.1. Experimental protocols

Hearts from Wistar rats were perfused in a non-circulating Langendorff apparatus with Krebs-Henseleit buffer gassed with 95% O_2 and 5% CO_2 at pH 7.4 and 37°C, and subsequently exposed to 40 min of global no-flow ischaemia followed by 15 min of reperfusion (*Figure 1*). Four hearts were assigned to each of the following four groups (*Figure 1*): (1) CTRL (control group), time-matched perfusion without ischaemia; (2) ISCH, test ischaemia followed by 15 min reperfusion; (3) PreC (pharmacological preconditioning) induced by isoflurane[18] administered for 15 min at 1.5 minimum alveolar concentration (1.5 MAC, corresponding to 2.1 vol%) and washed out for 10 min prior to test ischaemia; (4) PostC (pharmacological postconditioning) induced by 15 min isoflurane administration at 1.5 MAC right at the onset of reperfusion after test ischaemia. The buffer solution was equilibrated with isoflurane using an Isotec 3 vaporizer (Datex-Ohmeda, Tewksbury, MA, USA) with an air bubbler. Isoflurane concentrations were also measured in the buffer solution using a gas chromatograph (Perkin-Elmer, Norwalk, CT, USA): 0.54 ± 0.06 mM. Left ventricular developed pressure and coronary flow were recorded as previously described.[19]

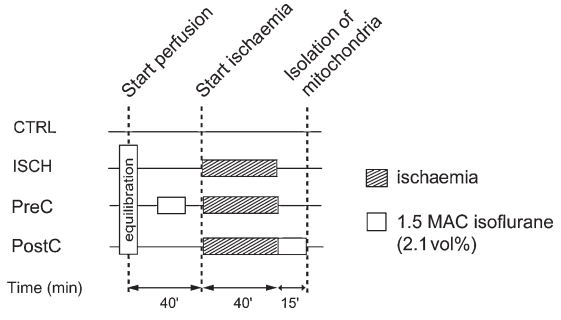

Figure 1 Scheme of treatment protocols. PreC: preconditioning with isoflurane (2.1 vol% for 15 min followed by 10 min of washout) prior to 40 min of test ischaemia. PostC: postconditioning with isoflurane (2.1 vol% during the first 15 min of reperfusion) after 40 min of test ischaemia. ISCH: non-preconditioned hearts exposed to 40 min of ischaemia. CTRL: time-matched perfusion. In each group, four hearts were used for analysis.

2.2. Isolation of mitochondria from rat heart tissue

Mitochondrial fractions were isolated as previously described.[20,21] Briefly, hearts were minced and homogenized in ice-cold homogenization buffer. After centrifugation, crude mitochondria were pelleted from the post-nuclear supernatant by centrifugation. The resultant supernatants were used as cytoplasmic fraction. Enriched mitochondria were resuspended in buffer, and purified in a 25% Percoll density gradient. After washing, mitochondrial proteins were solubilized and purity of the mitochondrial preparations was assessed by Western blotting using specific markers. The following antibodies were used: goat polyclonal anti-ANT antibody (N-19, Santa Cruz Biotechnology, USA), goat polyclonal anti-VDAC1 antibody (N-18, Santa Cruz Biotechnology), mouse monoclonal anti-NDUFS4 (MS104, MitoSciences, Eugene, OR, USA), rabbit polyclonal anti-sMtCK (a kind gift from Dr Theo Wallimann),[22] monoclonal mouse anti-calreticulin (BD Transduction Laboratories, Allschwil, Switzerland), polyclonal rabbit anti-catalase (Calbiochem, UK), and monoclonal anti-alpha tubulin (Sigma, St Louis, MO, USA).

2.3. Gel-based proteomics approach

Two-dimensional blue-native/sodium dodecyl sulphate gel electrophoresis (2D-BN-PAGE) was carried out as described by Schägger.[23] Western blotting was performed using monoclonal anti-phospho-Ser/Thr/Tyr antibody (SMP101, Assay Designs, LuBioScience, Switzerland).[24] Identification of gel spots was accomplished by matrix-assisted laser desorption/ionization-time of flight mass spectrometry (MALDI-TOF-MS).

2.4. Gel-free proteomics approach

After in-solution digestion, the peptide-containing solution was subjected to strong cation exchange chromatography and immobilized metal ion affinity chromatography for selective phosphopeptide enrichment. Phosphopeptides were identified by liquid chromatography-electrospray ionization-tandem mass spectrometry (LC-ESI-MS/MS) using linear ion trap-Fourier transform-ion cyclotron resonance and nanoflow reverse-phase high performance liquid chromatography separation followed by MALDI-TOF-MS/MS analysis.[25]

2.5. Immunoprecipitation

ANT protein was immunoprecipitated from purified rat heart mitochondrial fractions using goat polyclonal anti-ANT antibody (N-19, Santa Cruz Biotechnology, USA) coupled to protein G-sepharose (Amersham Biosciences).

2.6. Preparation of plasmids and yeast culture conditions

The *Ase*I and *BamH*I fragment of human ANT1 cDNA was amplified by polymerase chain reaction using pcDNA3-myc-ANT1 as a template, which was subcloned into *Nde*I and *BamH*I sites of pRS314-YA2P vector to generate pRS314-hANT1. The $hANT1^{Y194F}$ mutant was

generated using the QuickChange kit (Stratagene Europe, The Netherlands) and the mutagenic primers: 5′-CTACTTCGGAGTCTTTGATACTGC CAAGG-3′, and 5′-CCTTGGCAGTATCAAAGACTCCGAAGTAG-3′. The pRS314-YA2P vectors encoding hANT1 and hANT1^{Y194F} were transformed into the triple AAC-disrupted *Saccharomyces cerevisiae* JL-1-3 strain (*MAT*α *ade2-1 trp1-1 ura3-1 can1-100 aac1*::*LEU2 aac2*::*HIS3 aac3*::*URA*) by the lithium chloride method. Yeast strains were grown on plates containing fermentable (glucose) and non-fermentable (glycerol, lactate) carbon sources.

2.7. Statistics

For analysis of protein changes, unpaired *t*-tests of normalized spot intensities between groups were used. For analysis of haemodynamic data, unpaired *t*-test was used to compare groups at identical time points, and paired *t*-test to compare within groups over time (SigmaStat v 2.0; SPSS Science, Chicago, IL, USA). *P*-values $<$ 0.05 were considered significant.

3. Results

3.1. Effective myocardial protection and purity of mitochondrial fractions from rat hearts

Protection by isoflurane pre and postconditioning was confirmed by functional recovery and coronary flow measurements (see Supplementary material online, *Table S1*). The purity of mitochondrial fractions was carefully checked by Western blot analysis. *Figure 2* shows no contamination of the mitochondrial fraction (adenine nucleotide translocator, voltage-dependent anion channel 1, NADH dehydrogenase (ubiquinone) Fe-S protein 4, and sarcomeric mitochondrial creatine kinase) with cytosol (α-tubulin), endoplasmic reticulum (calreticulin), or peroxisome (catalase).

3.2. Differences in protein phosphorylation between protected (pre and postconditioned) vs. unprotected heart mitochondria

The BN-PAGE technique allows separation of hydrophobic protein complexes and provides information on their native interactions. The combination of BN-PAGE and SDS-PAGE techniques (2D-BN-PAGE) has become the method of choice for investigating the respiratory chain proteins in mitochondria and other hydrophobic protein complexes. As shown in *Figure 3*, only bands for the respiratory complexes I, II, III, IV, and V could be visualized on the first dimension of 2D-BN-PAGE. After SDS-PAGE, the subunits of each complex were resolved (see Supplementary material online, *Figure S1*). First, protein expression levels were compared and found unchanged between the four groups (data not shown). Next, protein phosphorylation was determined by immunoblotting using a phosphorylation-specific anti-phospho-Ser/Thr/Tyr antibody. With this approach, we could detect 61 phosphorylated protein spots per gel (*Figure 3*). All spots were subjected to MALDI-TOF-MS analysis, and 45 proteins were unequivocally identified and categorized into the following five groups: (1) oxidative phosphorylation (21 subunits); (2) tricarboxylic acid cycle (eight proteins); (3) fatty acid metabolism (11 subunits); (4) transport (three proteins); and (5) chaperones (two proteins; see *Table 1* for details). Some proteins displayed multiple spots generated by formation of different complexes, as observed with oxoglutarate dehydrogenase (OGDH), ubiquinol–cytochome *c* reductase complex core protein 2, aspartate aminotransferase (AST), dihydrolipoyllysine-residue succinyltransferase (component of OGDH), aconitate hydratase, malate dehydrogenase, short chain acetyl-CoA dehydrogenase, and adenine nucleotide translocator-1 (ANT1). Interestingly, six of the 61 protein spots were found to be ANT1 indicating that the abundant ANT1 protein forms various complexes in the inner mitochondrial membrane. To better compare the changes of phosphorylated protein spots, the mitochondrial proteins from different groups were first resolved on a 4–13% BN-PAGE. Subsequently, each gel lane was excised and cut into four parts, as indicated in *Figure 3*. Matched parts were assembled on the top of a 12% SDS gel and subjected to SDS-PAGE for the second dimension followed by Western blotting with the anti-phospho-Ser/Thr/Tyr antibody. Phosphorylation of 11 spots from seven proteins were found to be significantly changed (*Figure 4*). Phosphorylation

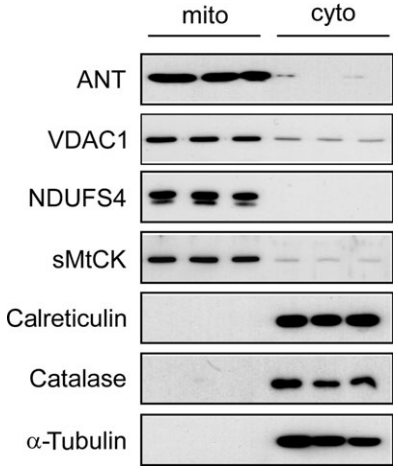

Figure 2 Purity of mitochondrial preparations. Mitochondrial and cytoplasmic fractions were immunoblotted with antibodies against adenine nucleotide transporter (ANT), a marker of the inner mitochondrial membrane, voltage-dependent anion channel 1 (VDAC1), a marker of the outer mitochondrial membrane, NDUFS4 [NADH dehydrogenase (ubiquinone) Fe-S protein], and sarcomeric mitochondrial creatine kinase (sMtCK); two other specific mitochondrial markers, calreticulin, a marker of the endoplasmic reticulum, catalase, a marker of peroxisomes, and the cytosolic marker α-tubulin.

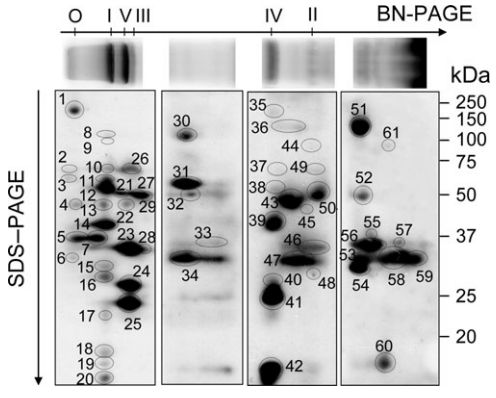

Figure 3 Separation of mitochondrial proteins by two-dimensional blue-native/sodium dodecyl sulphate gel electrophoresis (2D-BN-PAGE) and detection of phosphoproteins. Mitochondrial preparations were first resolved by 4–13% BN-PAGE. Gel slides were cut into four parts, as indicated, and matched parts were assembled on top of a 12% SDS gel for the second dimension SDS-PAGE followed by Western blot with anti-phospho-Ser/Thr/Tyr antibody. A total of 61 protein spots were found to be phosphorylated. Numbers refer to the protein identification presented in *Table 1*. Figure shows a representative 2D-BN-SDS gel of a control heart.

Table 1 Phosphoprotein spots identified by matrix-assisted laser desorption/ionization-time of flight mass spectrometry

Spot	Protein name	GI	Mr (kDa)	pI	Score	Reported phosphosites
Oxidative phosphorylation complex I						
8	NADH dehydrogenase (ubiquinone) Fe-S protein 1, 75 kDa	53850628	80.331	5.65	667	T611 (human)
11	NADH dehydrogenase (ubiquinone) flavoprotein 1	81883773	51.383	8.37	319	
12	NADH dehydrogenase (ubiquinone) Fe-S protein 2	58865384	52.927	6.52	1052	Y141 (human)
14	NADH-ubiquinone oxidoreductase 39 kDa subunit	81882598	41.900	9.77	354	
15	NADH-ubiquinone oxidoreductase 30 kDa subunit	23396786 (M)	30.360	6.40	85	
16	NADH-ubiquinone oxidoreductase 24 kDa subunit	83305118	27.703	6.23	48	
17	NADH dehydrogenase (ubiquinone) Fe-S protein 7	81883325	24.215	10.02	139	
18	NADH dehydrogenase (ubiquinone) 1 beta subcomplex subunit 6	94717662 (M)	15.374	9.79	87	
19	NADH dehydrogenase 1 beta 4, fragment	82617686	9.813	9.74	156	
20	NADH dehydrogenase (ubiquinone) 1 alpha subcomplex subunit 6	32363398 (M)	15.273	10.10	285	
Oxidative phosphorylation complex V						
23	ATP synthase gamma subunit, mitochondrial precursor	21263432 (M)	32.979	9.06	330	Y77 (bovine), S146 (mouse)
24	ATP synthase B chain, mitochondrial precursor	114625	28.965	9.39	872	
25	ATP synthase O subunit, mitochondrial precursor	20302061	23.440	10.03	603	Y35, Y46 (human)
26	ATP synthase, alpha subunit, mitochondrial precursor	83300587	55.218	8.28	118	S76 (mouse)
Oxidative phosphorylation, complex III						
21, 27,32	ubiquinol–cytochrome *c* reductase complex core protein 2	122066611	48.400	9.16	548	
28	cytochrome c-1	21759079 (M)	35.533	9.24	164	
Oxidative phosphorylation, complex IV						
40	cytochrome c oxidase subunit 3	117075	29.834	6.59	41	
41	cytochrome *c* oxidase subunit 2	117043	26.130	4.60	280	
42	cytochrome *c* oxidase subunit 4 isoform 1	117089	19.559	9.45	882	
Oxidative phosphorylation, complex II						
44	succinate dehydrogenase (ubiquinone) flavoprotein subunit	52782765	72.596	6.75	493	Y535, Y596 (rat)
48	succinate dehydrogenase complex subunit B (fragment)	89573817	27.377	8.33	261	
Tricarboxylic acid cycle						
38	Fumarate hydratase, mitochondrial precursor	120605	54.714	9.06	508	Y491 (human)
52	Citrate synthase	81902084	52.176	8.53	1561	Y80 (human)
1, 5, 35, 39	2-Oxoglutarate dehydrogenase E1 component (alpha-ketoglutarate dehydrogenase)	81883712	117.419	6.30	218	
2, 3	Dihydrolipoyllysine-residue succinyltransferase component of 2-oxoglutarate dehydrogenase complex	62512126	49.236	8.89	228	
4, 13, 22	Aspartate aminotransferase, mitochondrial precursor	112987	47.683	9.13	1544	Y96, Y401 (human)
36, 51	Aconitate hydratase, mitochondrial precursor	60391194	86.121	7.87	3476	Y71, Y544, Y655 (rat)
50	Isocitrate dehydrogenase (NADP), mitochondrial precursor	119364595	51.391	8.88	1868	
55, 56	Malate dehydrogenase	81878914 (M)	36.089	8.92	527	Y56, Y80 (human)
Lipids metabolism						
9	Propionyl-CoA carboxylase alpha chain	129684	78.289	6.33	268	S248 (mouse)
10	Propionyl-CoA carboxylase beta chain	129686	59.216	7.19	193	
30	Trifunctional enzyme subunit alpha, mitochondrial precursor	2494234	83.202	9.11	266	
31	Trifunctional enzyme subunit beta, mitochondrial precursor	2501192	51.667	9.50	934	
43	Long-chain specific acyl-CoA dehydrogenase, mitochondrial precursor	113016	48.242	7.63	2248	
45, 49	Acetyl-CoA dehydrogenase, short chain	81891723	45.224	8.47	851	

Continued

Table 1. *Continued*

Spot	Protein name	GI	Mr (kDa)	pI	Score	Reported phosphosites
46	2,4-Dienoyl-CoA reductase, mitochondrial precursor	67476443	36.395	9.08	388	
54	3,2-*trans*-enoyl-CoA isomerase, mitochondrial precursor	118210	32.348	9.55	918	
60	Short chain 3-hydroxyacyl-CoA dehydrogenase, mitochondrial precursor	7387725	34.540	8.83	1112	
61	Carnitine-*O*-palmitoyltransferase 2, mitochondrial precursor	117289	74.634	6.89	334	
Transport and other proteins						
33	Voltage-dependent anion-selective channel protein 1 (VDAC-1)	46397782	30.720	8.63	658	S13, Y67, S104, S137, Y195 (rat)
34, 47, 53, 57, 58, 59	ADP/ATP translocase 1 (adenine nucleotide translocator 1, ANT1)	461475	33.065	9.81	632	T83, Y190, Y194 (human ANT2)
29	Creatine kinase, sarcomeric mitochondrial precursor	125313	47.811	8.76	741	
37	*Mus musculus* solute carrier family 25 member 24	33286909	53.097	6.38	30	Y324 (human), Y322 (mouse)
Chaperones						

of cytochome *c* oxidase subunit 2 and OGDH were increased in groups subjected to ischaemia-reperfusion injury. In contrast, phosphorylation of NDUFA9, AST, 2,4-dienoyl-CoA reductase, prohibitin-2, and ANT1 were reduced in mitochondria from unprotected hearts (*Figure 4*).

3.3. Identification of novel phosphorylation sites in cardiac mitochondrial proteins

We identified 26 different phosphorylation sites in 19 proteins (*Table 2*). Twenty-four serine/threonine residues and two tyrosine residues were found. Except for malate dehydrogenase, aconitate hydratase, and ANT1, the other 16 proteins could not be found by 2D-BN-PAGE/Western blot with anti-phospho-Ser/Thr/Tyr antibody. Two of the 19 proteins contained two distinct phosphorylation sites, while one protein (pyruvate dehydrogenase E1 alpha subunit) contained six different sites. The exact position of the phosphorylated residues could not be assigned in three proteins. The MS/MS spectrum of ANT1, the major isoform of the ADP/ATP translocator in the heart, containing a phosphorylated tyrosine (Tyr^{194}), is depicted in *Figure 5*. Additional MS/MS spectra of identified phosphopeptides are shown as online supplemental data (see Supplementary material online, *Figure S2*).

3.4. Modulation of adenine nucleotide translocator phosphorylation by pre and postconditioning

The phosphorylation of ANT1 is of particular interest, as this protein is not only essential for the transport of ATP produced by oxidative respiration, but is also thought to be an integral component of the mitochondrial permeability transition pore.[6] To confirm the changes in ANT phosphorylation by pre and postconditioning, ANT protein was immunoprecipitated from all samples, and the phosphorylation of ANT was visualized by Western blot with anti-phospho-Tyr antibody. As shown in *Figure 6*, ANT phosphorylation was reduced after ischaemia-reperfusion alone (unprotected state). ANT dephosphorylation could be prevented by both protective therapies, i.e. preconditioning and postconditioning.

3.5. Yeast model reveals pivotal role of Tyr^{194} of adenine nucleotide translocator-1 in mitochondrial function

It is well-known that the ADP/ATP carriers (AACs), the yeast homologues of the mammalian ANT, are essential for oxidative phosphorylation, i.e. AAC-deficient yeast grows exclusively on fermentable media. Deletion of all the three AAC genes in yeast results in oxidative phosphorylation-deficient cells unable to grow on respiratory carbon sources (JL-1-3 strain). However, AAC-deficient yeast can grow in the presence of non-fermentable carbon sources, such as glycerol or lactate if expressing any of the three human ANT isoforms. Re-expression of human ANT1 restores growth of JL-1-3 yeast cells in both glycerol and lactate plates, as shown in *Figure 7*. To test whether phosphorylation at Tyr^{194} is required for yeast growth, we substituted Tyr^{194} by phenylalanine to create a non-phosphorylatable residue in ANT1 ($ANT1^{Y194F}$). Re-expression of the $ANT1^{Y194F}$ mutant into JL-1-3 yeast cells was unable to restore growth on non-fermentable carbon sources (*Figure 7*). Hence, loss of ANT phosphorylation at Tyr^{194} results in a defective oxidative growth phenotype.

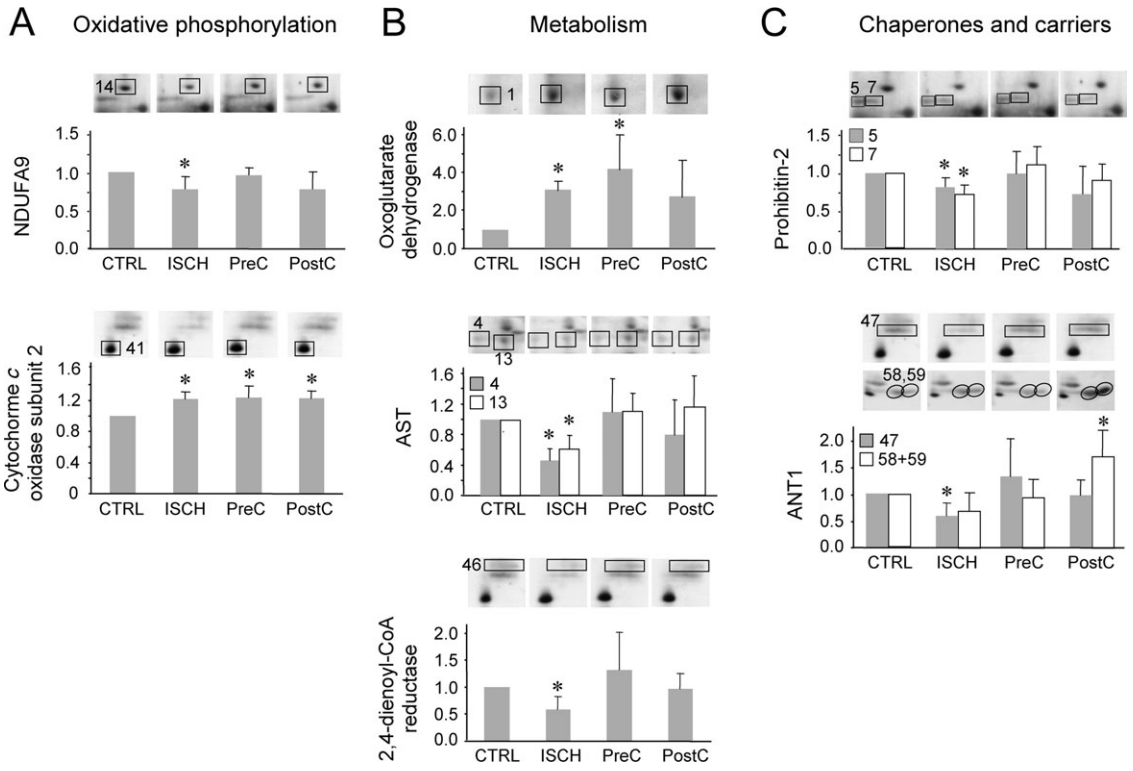

Figure 4 Differentially altered phosphoprotein spots, as identified by comparative two-dimensional blue-native/sodium dodecyl sulphate gel electrophoresis (2D-BN-PAGE) and Western blot analysis. Regions of 2D-blots with reproducible protein alterations were boxed, and the protein spots were identified by mass spectrometry. NDUFA9, NADH dehydrogenase ubiquinone 1 alpha subcomplex 9; AST, aspartate aminotransferase; ANT1, adenine nucleotide translocator-1. CTRL: time-matched perfusion; ISCH: hearts exposed to ischaemia-reperfusion; PreC, isoflurane preconditioning; PostC: isoflurane postconditioning. Data are mean $\pm$ SD ($n = 4$). Statistically significant changes relative to CTRL are indicated using two-tailed unpaired *t*-test: $^*P < 0.05$.

Similar results were obtained using a high expressing ANT1 vector (pRS424-hANT1; see Supplementary Material). Our results provide evidence for a potential role of Tyr^{194} in ANT1 in the context of cardioprotection.

4. Discussion

Our study focused on the systematic profiling of phosphoproteins in heart mitochondria. Since recent studies provide evidence that reversible phosphorylation of mitochondrial proteins is more common than previously expected,[14–17] and that this might be essential in the context of cardioprotection, we set out to assess the mitochondrial phosphoproteome in pre and postconditioned, i.e. protected heart mitochondria, and to compare this with the mitochondrial phosphoprotein profile of unprotected hearts. The ultimate goal was to identify novel anti-ischaemic targets. For this purpose, a gel-based approach, combining 2D-BN-PAGE,[23] Western blot analysis,[24] and MALDI-TOF-MS, and a gel-free phosphoproteomics approach including two phosphopeptide enrichment steps followed by LC-ESI-MS/MS or LC-MALDI-MS/MS[25] were used. The native gel-based method is widely used for both protein profiling and quantitative proteomic analyses, specifically for organelles like mitochondria, but it may suffer from difficulties in detecting low-abundance, very large, or small proteins. Using this technique, we identified a total of 61 phosphorylated proteins from rat heart mitochondria covering a wide range of key mitochondrial functions such as oxidative phosphorylation, tricarboxylic acid cycle, lipid metabolism, and transport or chaperone activities. For example, some oxidative phosphorylation units (NADH dehydrogenase Fe-S protein 7, NADH dehydrogenase 1 beta-4, ubiquinol–cytochrome *c* reductase complex core protein 2, cytochrome *c* oxidase subunit 4 isoform 1, and succinate dehydrogenase complex subunit B), and many of the proteins involved in lipid metabolism (propionyl-CoA carboxylase beta chain, trifunctional enzyme subunit alpha and beta, 2,4-dienoyl-CoA reductase, 3,2-*trans*-enoyl-CoA isomerase, short chain 3-hydroxyacyl-CoA dehydrogenase, and carnitine O-palmitoyltransferase 2) have not yet been reported to be phosphorylated in cardiac mitochondria. After selective enrichment of phosphopeptides and liquid chromatography followed by mass spectrometry, we were able to increase proteome coverage and to map 26 phosphorylation sites in 19 proteins. Many of the 26 identified phosphorylation sites in cardiac mitochondrial proteins are reported here for the first time.[26,27] Together, our observations suggest that phosphorylation may play a more prominent regulatory role in heart mitochondria than previously thought.

Although protective signalling pathways of pre and postconditioning converge at the mitochondrial level,[5,7] little is known about the post-translational modifications of possible end-effectors involved in cardioprotection. Recently, a number of protein kinases and phosphatases were found to colocalize with various mitochondrial sub-compartments,[9,11] but the ultimate targets of these kinases remain largely unknown. Using an isolated rabbit heart model, Kim *et al.*[28] compared the changes in protein expression of ischaemia-preconditioned mitochondria with non-preconditioned mitochondria and identified 25 differentially expressed mitochondrial proteins. Most of these proteins were related to

Table 2 Phosphopeptides and phosphorylation sites identified by LC-MS/MS analysis

Protein name	GI	Peptide sequence	Expect	Ion score	Observed mass	Charge	Phosphorylated residue	Instrument
Malate dehydrogenase	122065494	AGAG**S**ATLSMAYAGAR	3×10^{-7}	88	1535.68	2+	Ser-246[b]	LTQ-FT
Malate dehydrogenase	122065494	AGAG**S**ATLSMAYAGAR	2.6×10^{-5}	72	1534.67	1+	Ser-246[b]	MALDI
ADP/ATP translocase 1	461475	AAYFGV**Y**DTAK	0.0038	45	1286.56	2+	Tyr-194[b]	LTQ-FT
ADP/ATP translocase 1	461475	AAYFGV**Y**DTAK	0.00053	57	1285.54	1+	Tyr-194[b]	MALDI
Pyruvate dehydrogenase E1 component, alpha subunit	548409	YGMG**T**SVER	0.00065	48	1080.42	2+	Thr-231[b]	LTQ-FT
Pyruvate dehydrogenase E1 component, alpha subunit	548409	YGMG**T**SVER	7.5×10^{-6}	67	1080.42	2+	Ser-232	LTQ-FT
Pyruvate dehydrogenase E1 component, alpha subunit	548409	SMSDPGV**S**YR	0.0016	44	1179.46	2+	Ser-300	LTQ-FT
Pyruvate dehydrogenase E1 component, alpha subunit	548409	YGMG**T**SVER	0.041	37	1079.43	1+	Ser-232	MALDI
Pyruvate dehydrogenase E1 component, alpha subunit	548409	YGM*GT**S**VER	0.081	33	1095.41	1+	Ser-232	MALDI
Pyruvate dehydrogenase E1 component, alpha subunit	548409	**Y**GM*GTSVER	0.042	45	1095.41	1+	Tyr-227[b]	MALDI
Pyruvate dehydrogenase E1 component, alpha subunit	548409	YHGH**S**MSDPGV**S**YR	0.001	55	1753.64	3+	Ser-293 and Ser-300	LTQ-FT
Pyruvate dehydrogenase E1 component, alpha subunit	548409	YHGH**S**MSDPGVSYR	1.7×10^{-6}	73	1673.66	2+	Ser-293	LTQ-FT
Pyruvate dehydrogenase E1 component, alpha subunit	548409	YHGH**S**MSDPGV**S**YR	0.023	42	1752.61	1+	Ser-293 and Ser-300	MALDI
Succinyl-CoA ligase (ADP-forming), beta-chain	52788305	INFD**S**NSAYR	0.00032	53	1267.52	2+	Ser-279	LTQ-FT
Succinyl-CoA ligase (ADP-forming), beta-chain	52788305	INFD**S**NSAYR	5.2×10^{-6}	76	1266.51	1+	Ser-279	MALDI
Ubiquinol-cytochrome c reductase complex 11 kDa protein	62511137	ERLE**S**CDRR	0.035	29	1300.54	1+	Ser-50[b]	MALDI
Ubiquinol-cytochrome c reductase complex 11 kDa protein	62511137	ERLE**S**CDR	0.04	25	1144.47	1+	Ser-50[b]	MALDI
NADH dehydrogenase (ubiquinone) flavoprotein 3-like isoform 1	162287192	DSSSSSSSSSSDSDSDGEEHGSDIGPR[a]	2×10^{-8}	100	2738.05	1+	ND[b]	MALDI
Enoyl-CoA hydratase	119119	AVGKSLAM*EMVL**T**GDR	0.01	33	1773.84	1+	Thr-194[b]	MALDI
Aconitate hydratase	60391194	WVVIGDENYGEG**S**SR	0.03	42	1747.7	1+	Ser-669[b]	MALDI
Glycerol 3-phosphate acyltransferase, mitochondrial	8393466	WKESLM**S**R	0.012	35	1116.53	1+	Ser-57[b]	MALDI
Glycerol 3-phosphate acyltransferase, mitochondrial	8393466	SDEEDED**S**DFGEEQR	1.1×10^{-5}	71	1866.65	1+	Ser-695	MALDI
2-oxoisovalerate dehydrogenase subunit alpha, mitochondrial precursor	129032	IGHH**S**TSDDSSAYR	1.2×10^{-7}	92	1612.6	1+	Ser-337	MALDI
2-oxoisovalerate dehydrogenase subunit alpha, mitochondrial precursor	129032	**S**VDEVNYWDK	1.5×10^{-5}	72	1334.54	1+	Ser-343	MALDI
3-methyl-2-oxobutanoate dehydrogenase kinase	3183508	*ST*SATDTHHVELAR[a]	4.2×10^{-9}	108	1604.67	1+	Ser-31 or Thr-32[b]	MALDI
TOM70 homologue A	47058988	A**S**PALGSGPDGSGDSLEM*SSLDR	2.2×10^{-5}	71	302.04	1+	Ser-94	MALDI
A kinase anchor protein 1, mitochondrial precursor	13959285	RR**S**ESSGNLPSIVDTR	0.03	37	1853.9	1+	Ser-101	MALDI
BCL2/adenovirus E1B 19 kDa protein-interacting protein 3	6093508	NSTL**S**EEDYIER	7×10^{-6}	76	1535.65	1+	Ser-88	MALDI
Mitochondrial aspartate glutamate carrier 1 (solute carrier family 25, member 12)	13124050	DVEVTKEEFAQ**S**AIR	0.01	21	1801.88	1+	Ser-256[b]	MALDI
heat shock 27 kDa protein 1	94400790	SP**S**WEPFR	0.0024	47	1085.4	1+	Ser-15	MALDI
similar to CG31759-PA	81884455	SPAEA*TT*HEAVR[a]	0.04	38	1348.67	1+	Thr-26 or Thr-27[b]	MALDI
hypothetical protein	123780395	DADEED**S**DEETSHLER	1.6×10^{-8}	102	1956.79	1+	Ser-106[b]	MALDI
regulator of microtubule dynamics 3	62078823	SQ**S**LPNSLDYAQTSER	0.00015	63	1875.86	1+	Ser-46[b]	MALDI

The phosphorylation sites are bold and oxidized methionines are denoted by the '*' symbol. GI denotes GenInfo Identifier (GenBank).

[a]The exact position of the phosphorylated residue cannot be assigned. Phosphorylation sites were verified against either PhosphoSitePlus (http://www.phosphosite.org/homeAction.do) or Phospho.ELM (http://phospho.elm.eu.org/index.html) databases, accessed February 25, 2008.

[b]Novel phosphorylation sites.

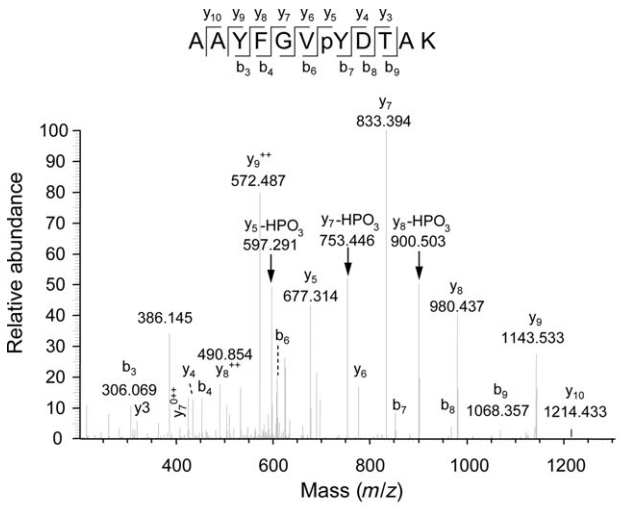

#	b	b++	b0	b0++	Seq	y	y++	y*	y*++	y0	y0++	#
1	72.04	36.53			A							11
2	143.08	72.04			A	1214.51	*607.76*	1197.49	599.25	1196.50	598.75	10
3	*306.14*	153.58			Y	*1143.48*	*572.24*	1126.45	563.73	1125.47	563.24	9
4	*453.21*	227.11			F	*980.41*	*490.71*	963.39	482.20	962.40	481.70	8
5	510.23	255.62			G	*833.34*	417.18	816.32	*408.66*	815.33	*408.17*	7
6	*609.30*	305.16			V	*776.32*	388.66	759.30	380.15	758.31	379.66	6
7	*852.33*	426.67			Y	*677.25*	339.13	660.23	330.62	659.24	330.13	5
8	*967.36*	484.18	949.35	475.18	D	*434.22*	217.62	417.20	209.10	416.21	208.61	4
9	*1068.41*	534.71	1050.40	525.70	T	*319.20*	160.10	302.17	151.59	301.19	151.10	3
10	1139.44	570.23	1121.43	561.22	A	218.15	109.58	201.12	101.07			2
11					K	147.11	74.06	130.09	65.55			1

Figure 5 MS/MS spectrum of the tyrosine phosphopeptide (Y^{194}) of adenine nucleotide translocator-1 (ANT1). Precursor ion mass and MS/MS were measured in LTQ-FT mass-spectrometer. Arrows indicate phosphate loss in the indicated ions. The measured masses of b- and y-ions are in italic.

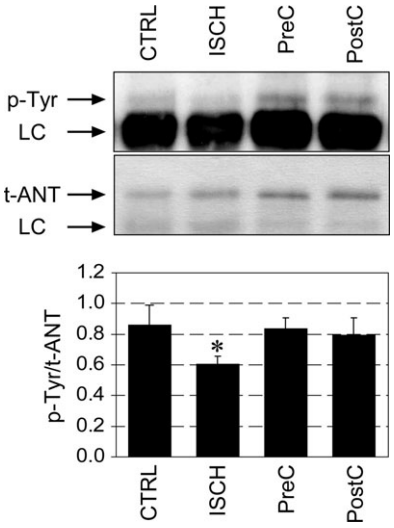

Figure 6 Phosphorylation of adenine nucleotide translocator (ANT) in heart mitochondria. ANT protein was immunoprecipitated from 50 μg of purified rat heart mitochondrial fractions and subjected to Western blot with anti-phospho-tyrosine antibody. Representative Western blots (upper) and averaged density data of phosphorylated tyrosine of ANT (p-Tyr) compared with total ANT (t-ANT) are shown for each group. IgG LC: light chain of goat ANT antibody; CTRL: time-matched perfusion; ISCH: hearts exposed to ischaemia-reperfusion alone; PreC, isoflurane preconditioning; PostC: isoflurane postconditioning. Data are mean ± SD ($n = 4$). *$P < 0.05$ vs. ISCH.

respiratory chain and energy metabolism. In another study by Arrell *et al.*,[29] isolated rabbit cardiomyocytes were preconditioned with adenosine and diazoxide, but no index ischaemia was applied. After 2 h of drug exposure, whole cell lysates were collected and subjected to 2D-gel electrophoresis. This study identified 28 differentially expressed protein spots, the majority of which again was involved in bioenergetics. Interestingly, the same study also found four new phosphorylation sites, one at the β-subunit of ATP-synthase. While both studies predominantly focused on changes in protein expression, fundamental changes in heart physiology may typically occur without changes in protein abundance but rather in response to post-translational modifications such as phosphorylation. Comparing the phosphorylation profiles of protected vs. unprotected mitochondria, we were able to identify seven proteins from 11 spots that were differentially phosphorylated. Phosphorylation of cytochrome *c* oxidase subunit 2 and OGDH were increased in protected and unprotected mitochondria, suggesting that phosphorylation of these proteins may be related to ischaemia-reperfusion injury. In contrast, phosphorylation of NDUFA9, AST, 2,4-dienoyl-CoA reductase, prohibitin-2, and ANT1 were exclusively reduced by ischaemia-reperfusion alone, but largely unaffected by both pre and postconditioning. Hence, phosphorylation of these sites may be rather linked to cardioprotection.

To test whether the observed phosphorylation of ANT1 was indeed linked to biological significance and to exclude the possibility of mere association or experimental artefacts, we determined the biological significance of the novel phosphorylation site of ANT1 at residue Tyr^{194}. ANT, called AAC in yeast, is the most abundant protein of the inner mitochondrial membrane and belongs to the mitochondrial solute carrier family involved in a variety of transport activities across the inner mitochondrial membrane.[30] ANT facilitates the exchange of ADP/ATP by an antiport mechanism and thus is essential for the utilization of ATP produced by oxidative phosphorylation. Moreover, ANT is thought to be an integral component of the mitochondrial permeability transition pore (mPTP),[19] albeit this function is still under debate.[31] Current evidence suggests that cardioprotection by pre and postconditioning is ultimately mediated through the inhibition of mitochondrial permeability transition. Baines *et al.*[32] reported that PKCε closely interacts with cardiac mitochondria implying that components of the mPTP complex might be the principal target of this kinase. In our study, we could show that ischaemia-induced ANT dephosphorylation could be prevented or reversed by both pre and postconditioning. A major phosphorylation site of ANT was identified on Tyr^{194}, which is the last of three tyrosines $Tyr^{186}/Tyr^{190}/Tyr^{194}$ forming a ladder along the transmembrane helix H4 oriented towards the cavity of the channel.[30,33] A 'stacking interaction' with the tyrosine rings could guide the nucleotides along this tyrosine ladder, and phosphorylation of Tyr^{194} could markedly interfere with or modulate the process. Intriguingly, in yeast we could show that mutation of Tyr^{194} to Phe, mimicking the non-phosphorylated state, failed to rescue cellular growth on a non-fermentable carbon source when transforming the human ANT1 into the AAC-deficient yeast strain JL-1-3. Therefore, our results provide evidence that this phosphorylation site is critical for mitochondrial bioenergetics, which is in accordance with the previous reports showing that tyrosine phosphorylation of

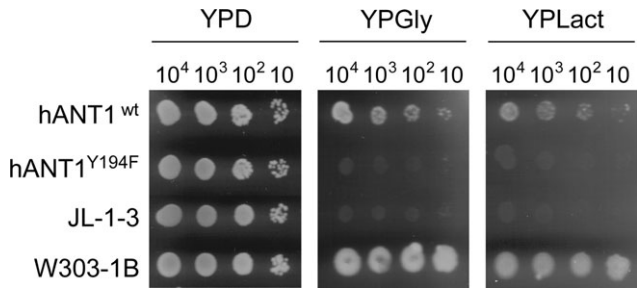

Figure 7 Yeast growth on fermentable and non-fermentable substrates. The *Saccharomyces cerevisiae* strain JL-1-3 was transformed with pRS314-YA2P encoding human ANT1 wild-type and ANT1^{Y194F}. Transformants were plated on yeast extract peptone dextrose, YPGly, and YPLact plates. After three days of incubation at 28°C on yeast extract peptone dextrose and seven days on YPGly and YPLact, the plates were photographed. W303-1B denotes haploid strain of *S. cerevisiae*.

mitochondrial proteins is enhancing ATP production.[34] Although the yeast experiments extend our proteomic findings from isolated rat hearts showing that Tyr194 phosphorylation of ANT1 is associated with cardioprotection, future experiments using hypoxia/reoxygenation will have to prove this concept in mammalian cells.

In our comparative phosphoproteomics study, we used 2D-BN-PAGE-coupled Western blotting with an antibody specific for phospho-Ser/Thr/Tyr. Although this approach is comparable with those using fluorescent phosphosensor dyes (ProQ Diamond dye), it is conceivable that some phosphoproteins may remain undetected by either methods.[35] In addition, some proteins may be dephosphorylated during the mitochondria isolation process or even during BN-PAGE. Because of the lack of antibodies, we were unable to confirm all the observed changes in phosphorylation by immunoprecipitation. Besides phosphorylation, we found other modifications in mitochondrial proteins. For example, tryptophan modifications (kynurenine and formylkynurenine), which have a profound impact on cell death and survival and are implicated in a number of pathologies,[36] were frequently observed in our study (data not shown). This is not so much surprising since mitochondrial proteins are exposed to high amounts of reactive oxygen species. In addition, histidine[37] and cysteine[38] phosphorylation was also observed (His^{292} of pyruvate dehydrogenase E1 alpha subunit and Cys^{63} of sarcomeric mitochondrial creatine kinase). Although histidine and cysteine phosphorylation were previously reported, their physiological relevance remains largely unknown. In the current study, the halogenated ether isoflurane was used to elicit pre and postconditioning in hearts. This class of drugs was proven to be of value in the clinical setting of patients undergoing coronary artery bypass grafting surgery.[39,40] However, it is possible that other pre and postconditioning mimicking agents may elicit different phosphoprotein profiles in heart mitochondria.

In summary, our comparative analysis of mitochondrial phosphoproteins in pre and postconditioned, i.e. protected vs. unprotected mitochondria, revealed a total of 61 phosphoproteins including 26 phosphorylation sites and it proved to be an effective approach for elucidating the molecular events underlying ischaemic injury and protective mechanisms. A major phosphorylation site was identified in ANT1 at Tyr^{194}. The substitution of this site with Phe, mimicking the non-phosphorylated state, resulted in the complete inhibition of oxidative growth in the yeast model suggesting that phosphorylation at this novel site is critical for bioenergetics and may thus substantially contribute to cardioprotection.

Supplementary material

Supplementary material is available at *Cardiovascular Research* online.

Funding

Swiss National Science Foundation, Berne, Switzerland (3200B0-103980/1, 3200B0-116110/1 to M.Z.); Swiss University Conference, Berne, Switzerland (to M.Z. and M.C.S.); EMDO Foundation, Zurich, Switzerland (to M.Z.), Abbott Research Grant Switzerland, Baar, Switzerland (to M.Z.); Olga Mayenfisch Foundation, Zurich, Switzerland (to M.Z.); fifth Frontiers in Anesthesia Research Award, International Anesthesia Research Society, Cleveland, USA (to M.Z.).

Conflict of interest: none declared.

References

1. Murry CE, Jennings RB, Reimer KA. Preconditioning with ischemia: a delay of lethal cell injury in ischemic myocardium. *Circulation* 1986;**74**:1124–1136.
2. Zaugg M, Schaub MC. Signaling and cellular mechanisms in cardiac protection by ischemic and pharmacological preconditioning. *J Muscle Res Cell Motil* 2003;**24**:219–249.
3. Zhao ZQ, Corvera JS, Halkos ME, Kerendi F, Wang NP, Guyton RA *et al*. Inhibition of myocardial injury by ischemic postconditioning during reperfusion: comparison with ischemic preconditioning. *Am J Physiol Heart Circ Physiol* 2003;**285**:H579–H588.
4. Hausenloy DJ, Yellon DM. Survival kinases in ischemic preconditioning and postconditioning. *Cardiovasc Res* 2006;**70**:240–253.
5. Juhaszova M, Zorov DB, Kim SH, Pepe S, Fu Q, Fishbein KW *et al*. Glycogen synthase kinase-3beta mediates convergence of protection signaling to inhibit the mitochondrial permeability transition pore. *J Clin Invest* 2004;**113**:1535–1549.
6. Murphy E, Steenbergen C. Preconditioning: the mitochondrial connection. *Annu Rev Physiol* 2007;**69**:51–67.
7. Murphy E. Primary and secondary signaling pathways in early preconditioning that converge on the mitochondria to produce cardioprotection. *Circ Res* 2004;**94**:7–16.
8. Di Lisa F, Canton M, Menabo R, Kaludercic N, Bernardi P. Mitochondria and cardioprotection. *Heart Fail Rev* 2007;**12**:249–260.
9. Pagliarini DJ, Dixon JE. Mitochondrial modulation: reversible phosphorylation takes center stage? *Trends Biochem Sci* 2006;**31**:26–34.
10. McBride HM, Neuspiel M, Wasiak S. Mitochondria: more than just a powerhouse. *Curr Biol* 2006;**16**:R551–R560.
11. Salvi M, Brunati AM, Toninello A. Tyrosine phosphorylation in mitochondria: a new frontier in mitochondrial signaling. *Free Radic Biol Med* 2005;**38**:1267–1277.
12. Ping P, Zhang J, Zheng YT, Li RC, Dawn B, Tang XL *et al*. Demonstration of selective protein kinase C-dependent activation of Src and Lck tyrosine kinases during ischemic preconditioning in conscious rabbits. *Circ Res* 1999;**85**:542–550.
13. Wilson JE. Isozymes of mammalian hexokinase: structure, subcellular localization and metabolic function. *J Exp Biol* 2003;**206**:2049–2057.
14. Palmisano G, Sardanelli AM, Signorile A, Papa S, Larsen MR. The phosphorylation pattern of bovine heart complex I subunits. *Proteomics* 2007;**7**:1575–1583.
15. Augereau O, Claverol S, Boudes N, Basurko MJ, Bonneu M, Rossignol R *et al*. Identification of tyrosine-phosphorylated proteins of the mitochondrial oxidative phosphorylation machinery. *Cell Mol Life Sci* 2005;**62**:1478–1488.
16. Hopper RK, Carroll S, Aponte AM, Johnson DT, French S, Shen RF *et al*. Mitochondrial matrix phosphoproteome: effect of extra mitochondrial calcium. *Biochemistry* 2006;**45**:2524–2536.
17. Lewandrowski U, Sickmann A, Cesaro L, Brunati AM, Toninello A, Salvi M. Identification of new tyrosine phosphorylated proteins in rat brain mitochondria. *FEBS Lett* 2008;**582**:1104–1110.

18. Zaugg M, Lucchinetti E, Spahn DR, Pasch T, Schaub MC. Volatile anesthetics mimic cardiac preconditioning by priming the activation of mitochondrial K(ATP) channels via multiple signaling pathways. *Anesthesiology* 2002;**97**:4–14.
19. Feng J, Lucchinetti E, Ahuja P, Pasch T, Perriard JC, Zaugg M. Isoflurane postconditioning prevents opening of the mitochondrial permeability transition pore through Inhibition of glycogen synthase kinase 3beta. *Anesthesiology* 2005;**103**:987–995.
20. O'Gorman E, Beutner G, Wallimann T, Brdiczka D. Differential effects of creatine depletion on the regulation of enzyme activities and on creatine-stimulated mitochondrial respiration in skeletal muscle, heart, and brain. *Biochim Biophys Acta* 1996;**1276**:161–170.
21. Walzel B, Speer O, Zanolla E, Eriksson O, Bernardi P, Wallimann T. Novel mitochondrial creatine transport activity. Implications for intracellular creatine compartments and bioenergetics. *J Biol Chem* 2002;**277**: 37503–37511.
22. Schlattner U, Mockli N, Speer O, Werner S, Wallimann T. Creatine kinase and creatine transporter in normal, wounded, and diseased skin. *J Invest Dermatol* 2002;**118**:416–423.
23. Schägger H. Blue-native gels to isolate protein complexes from mitochondria. *Methods Cell Biol* 2001;**65**:231–244.
24. Kimura M, Mizukami Y, Miura T, Fujimoto K, Kobayashi S, Matsuzaki M. Orphan G protein-coupled receptor, GPR41, induces apoptosis via a p53/Bax pathway during ischemic hypoxia and reoxygenation. *J Biol Chem* 2001;**276**:26453–26460.
25. Munton RP, Tweedie-Cullen R, Livingstone-Zatchej M, Weinandy F, Waidelich M, Longo D *et al*. Qualitative and quantitative analyses of protein phosphorylation in naive and stimulated mouse synaptosomal preparations. *Mol Cell Proteomics* 2007;**6**:283–293.
26. Hornbeck PV, Chabra I, Kornhauser JM, Skrzypek E, Zhang B. PhosphoSite: a bioinformatics resource dedicated to physiological protein phosphorylation. *Proteomics* 2004;**4**:1551–1561.
27. Diella F, Gould CM, Chica C, Via A, Gibson TJ. Phospho.ELM: a database of phosphorylation sites–update 2008. *Nucleic Acids Res* 2008;**36**: D240–D244.
28. Kim N, Lee Y, Kim H, Joo H, Youm JB, Park WS *et al*. Potential biomarkers for ischemic heart damage identified in mitochondrial proteins by comparative proteomics. *Proteomics* 2006;**6**:1237–1249.
29. Arrell DK, Elliott ST, Kane LA, Guo Y, Ko YH, Pedersen PL *et al*. Proteomic analysis of pharmacological preconditioning: novel protein targets converge to mitochondrial metabolism pathways. *Circ Res* 2006;**99**:706–714.
30. Nury H, Dahout-Gonzalez C, Trezeguet V, Lauquin GJ, Brandolin G, Pebay-Peyroula E. Relations between structure and function of the mitochondrial ADP/ATP carrier. *Annu Rev Biochem* 2006;**75**:713–741.
31. Kokoszka JE, Waymire KG, Levy SE, Sligh JE, Cai J, Jones DP *et al*. The ADP/ATP translocator is not essential for the mitochondrial permeability transition pore. *Nature* 2004;**427**:461–465.
32. Baines CP, Song CX, Zheng YT, Wang GW, Zhang J, Wang OL *et al*. Protein kinase Cepsilon interacts with and inhibits the permeability transition pore in cardiac mitochondria. *Circ Res* 2003;**92**:873–880.
33. Pebay-Peyroula E, Dahout-Gonzalez C, Kahn R, Trezeguet V, Lauquin GJ, Brandolin G. Structure of mitochondrial ADP/ATP carrier in complex with carboxyatractyloside. *Nature* 2003;**426**:39–44.
34. Pagliarini DJ, Wiley SE, Kimple ME, Dixon JR, Kelly P, Worby CA *et al*. Involvement of a mitochondrial phosphatase in the regulation of ATP production and insulin secretion in pancreatic beta cells. *Mol Cell* 2005;**19**: 197–207.
35. McDonald T, Sheng S, Stanley B, Chen D, Ko YH, Cole RN *et al*. Expanding the subproteome of the inner mitochondria using protein separation technologies: one- and two-dimensional liquid chromatography and two-dimensional gel electrophoresis. *Mol Cell Proteomics* 2006;**5**:2392–2411.
36. Hunzinger C, Wozny W, Schwall GP, Poznanovic S, Stegmann W, Zengerling H *et al*. Comparative profiling of the mammalian mitochondrial proteome: multiple aconitase-2 isoforms including N-formylkynurenine modifications as part of a protein biomarker signature for reactive oxidative species. *J Proteome Res* 2006;**5**:625–633.
37. Klumpp S, Krieglstein J. Reversible phosphorylation of histidine residues in vertebrate proteins. *Biochim Biophys Acta* 2005;**1754**:291–295.
38. Guan KL, Dixon JE. Evidence for protein-tyrosine-phosphatase catalysis proceeding via a cysteine-phosphate intermediate. *J Biol Chem* 1991; **266**:17026–17030.
39. Julier K, da Silva R, Garcia C, Bestmann L, Frascarolo P, Zollinger A *et al*. Preconditioning by sevoflurane decreases biochemical markers for myocardial and renal dysfunction in coronary artery bypass graft surgery: a double-blinded, placebo-controlled, multicenter study. *Anesthesiology* 2003;**98**:1315–1327.
40. Lucchinetti E, Hofer C, Bestmann L, Hersberger M, Feng J, Zhu M *et al*. Gene regulatory control of myocardial energy metabolism predicts postoperative cardiac function in patients undergoing off-pump coronary artery bypass graft surgery: inhalational versus intravenous anesthetics. *Anesthesiology* 2007;**106**:444–457.